Smart Solutions in Smart Spaces: Getting the Most from Far-Field Wireless Power Transfer

HOW TO GET THE MOST FROM FAR-FIELD WIRELESS POWER TRANSFER

Alessandra Costanzo, and Diego Masotti

Alessandra Costanzo (alessandra.costanzo@unibo.it) and Diego Masotti (diego.masotti@unibo.it) are with the Alma Mater Studiorum University of Bologna, Department of Electrical, Electronic and Information Engineering – Guglielmo Marconi – Bologna, ITALY.

Motivation

Nowadays there is an almost unlimited number of monitoring applications, such as structural health, logistic, security, healthcare and agriculture, which are planning to be based on a large deployment of co-operative wireless microsystems, with sensing capabilities, moving closer to the effective realization of the paradigm of the Internet of Things.

The main open challenge is the reliability of maintenance-free devices, with life-time duration, especially from the energy sustainability point of view. Such systems are required to power themselves, by harvesting energy from the ambient, thus eliminating battery needs. To minimize energy requirements, wake-up radios able to be activated by signals as low as -50 dBm are already available [1]. RF/microwave energy sources are foreseen as one of the best candidates to comply with energy autonomy, either because they are widely distributed in humanized environments or because they can be efficiently provided on demand. These two different ways of providing RF energy can be referred to as RF energy harvesting (EH) and wireless power transmission (WPT), respectively. In both cases a delicate design of the RF power transfer link, consisting of the nonlinear sub-systems and the radiating elements, is required, providing that their characteristics are carefully optimized depending on the particular contest and scenario.

Intensive industrial and academic activities has been devoted to this field: several and concurrent techniques and circuit solutions have been proposed and tested to ensure non-intermittent, sufficient wireless power transfer, with the lowest possible density. In this way, it is possible to comply with maximum transfer efficiency and minimum EM interference and pollution, at the same time.

Typical frequencies adopted for these purposes are in the UHF and SHF bands around 400-800 MHz, for terrestrial TV signals, and around 900, 1800, 2400 and 5800 MHz, for different wireless standards: since the geometrical area to be covered are usually of the order of few meters, the devices to be powered are in the far-field region of their known or unknown RF/microwave sources.

This article reviews some of the recent and promising circuit and antenna solutions and discusses reliable sub-systems adopted for receiving and transmitting subsystems, their associated radiating elements, with a focus on minimizing the power budget for enabling device operations.

Block representation of a far-field power transfer system

Fig. 1 shows a block chain representation of an entire far-field wireless power system from the transmitter dc bias to the receiver dc output: it consists of a power source connected to a transmitting antenna system, the radio channel, a receiving antenna system connected to a rectifier circuit whose dc output is managed by a dc-to-dc converter that provides the energy to the battery-less device [2, 3]. The significant power quantities to be monitored, at each subsystem connecting ports, are also outlined in Fig. 1. The exact knowledge of these quantities can be used to compute the entire system efficiency, as a product of the following ratios:

$$\eta_{TOT} = \eta_{BIAS-RF} \cdot \eta_{RF-RF} \cdot \eta_{RF-DC} \cdot \eta_{DC-DC} = \frac{P_{TX}}{P_{BIAS}} \cdot \frac{P_{RX}}{P_{TX}} \cdot \frac{P_{DC}}{P_{RX}} \cdot \frac{P_{ST}}{P_{DC}} \quad (1)$$

where, P_{BIAS} is the dc power required at the transmitter side, P_{TX} is the RF power available at the transmitting antenna input port, P_{RX} is the RF power received by the antenna, P_{DC} is the rectifier output power, and P_{ST} is the dc-to-dc converter output power. Of course, all these quantities are dependent on the operating frequencies and on the power densities involved, due to the nonlinear nature of the link building blocks. The first factor is the dc-to-RF conversion efficiency of the power source. The second one accounts for the transmitting and receiving antennas performances and the radio channel multipath and fading effects, which are linear but frequency-dependent and determine the geometrical range that can be covered by the RF source. A rigorous circuit equivalent model formulation to accurately evaluate this contribution can be derived by EM theory [4]. The third factor is the RF-to-dc conversion efficiency of the rectifier. The last factor is the dc-to-dc conversion efficiency of a power management unit that is optimized to dynamically track the rectifier optimum load. Since the entire WPT system consists of a connection of nonlinear circuits, its behavior is strongly dependent on the power levels involved, on the RF sources waveforms and operating frequencies and can be precisely quantified only if such blocks behaviors are exactly known.

Furthermore, (1) can be exactly evaluated only in case of intentional WPT sources, whereas it is not possible in energy harvesting scenarios where ambient available RF sources are exploited. For energy scavenging purposes, the transmitter side is not under control, but the available RF sources distributed in the ambient are used. Thus, only the RF behavior of the rectifier and the baseband operation of the PMU can be optimized using a realistic estimation of the available power densities, such as those provided in [5-9].

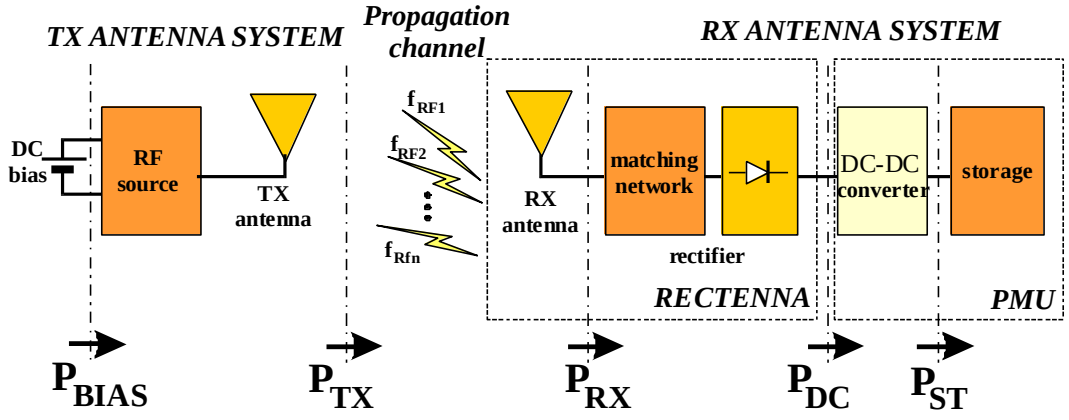

Fig. 1: Building blocks of a far-field wireless power transfer system and power quantities involved.

Wireless powering on demand and from the ambient

The two different scenarios for wirelessly powering are schematically depicted in Fig. 2 and 3 and will be referred as wireless powering from ambient RF energy, or energy harvesting (EH), and wireless powering on demand (WPT), respectively. The EH scenarios of Fig. 2 shows devices scavenging energy from RF sources, randomly present in the environment at different operating frequencies, such as TV, WiFi and cell phone standards. In this case the available energy is ambient-dependent and highly time-variable. Furthermore the transmitter side performance, such as the dc-to-RF conversion efficiency, the RF output power and the antenna radiation behaviour are not available and can only be roughly estimated. The same is true for the knowledge of the radio channel. Thus the RF receiver side, commonly referred as *rectenna* (rectifying antenna) must be designed to comply with these uncertainties and the antennas should feature broadband or multi-band behaviours, to cover all the wireless standards available in the ambient, with circular or dual polarization, to ensure signal reception in any link conditions. Since the ultimate target is to scavenge all RF sources at the same time, at any possible frequency, polarization, angle of arrival and power intensity, it is apparent that the design of such harvesting systems is a very demanding task. Furthermore, it has been proven [5-9] that the available ambient RF power density is usually very low, ranging from few nW/cm^2 to few μW/cm^2, and highly-efficient (resonant) antennas as well as carefully optimized rectifier are needed . Finally, since such radiating systems are needed to be integrated in low-weighted miniaturized devices, a compromise between performance and optimum size is necessary.

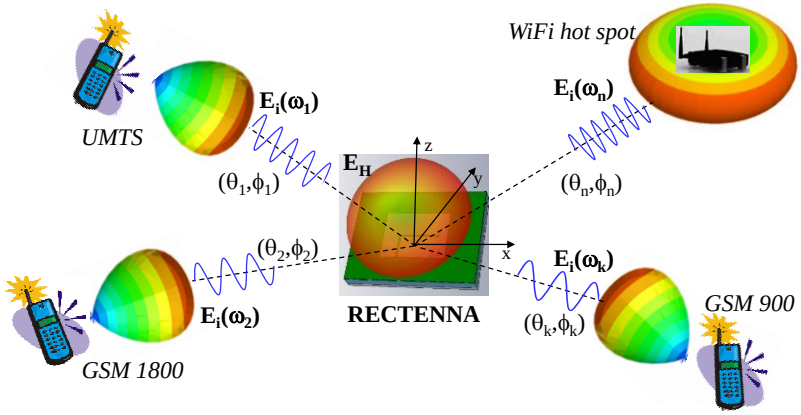

Fig. 2: Energy harvesting scenario in presence of multiple, randomly distributed RF sources [3].

In Fig. 3 a wireless power transfer scenario with dedicated known RF sources, is schematically shown. With this configuration the receiving system design takes advantage of the knowledge of the RF frequencies, the direction of arrival and polarization of the incident power. For example, dedicated Radio Frequency (RF) sources, ready to provide the necessary (low) energy when requested [3], may be installed. This case is similar to powering passive RF Identification (RFID) tags. In such situation a different design approach from the previous one should be followed, since any WPT system building block can be deterministically predicted and the available power densities, at the battery-less devices location, can be more accurately evaluated. Directive, single band, resonant antennas, with polarizations coherent with those of the transmitting side,

can be used and the overall system efficiency can be precisely maximized. Later in this article, it will be shown that in such situation power density minimization can be obtained by exploiting optimized transmitted signal waveforms and smart beaming strategies to focus the energy on demand.

Thus adopting dedicated RF sources is foreseen as the most promising choice for the effective implementation of the IoT scenarios, because from one hand it allows a precise knowledge of the energy availability, thus ensuring the safe range for devices powering, from the other hand such energy can be focused and provided in such a way that the receiver side efficiency is enhanced.

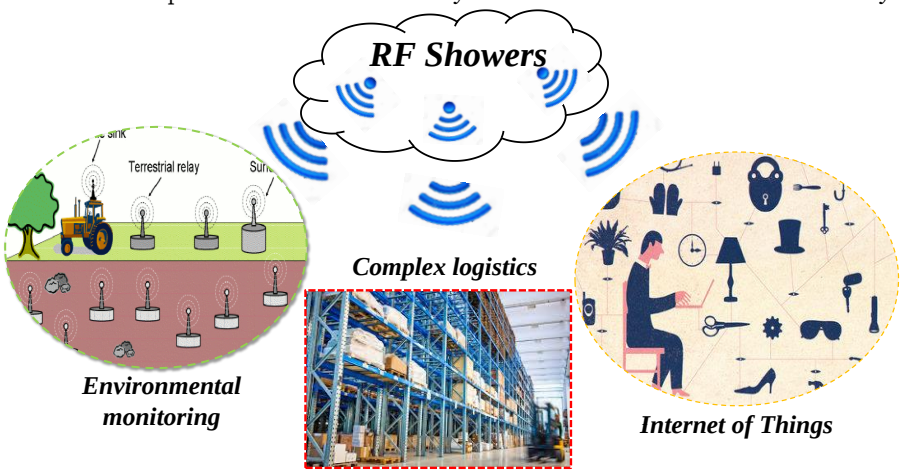

Fig. 3: Wireless power transfer scenario with dedicated known RF sources

The design features, the degrees of freedom and the available information for wireless powering from the ambient and for the intentional wireless powering are summarized in Tables I and II, respectively.

WIRELESS POWERING FROM THE AMBIENT		
TRANSMITTER SIDE (TX)	POWER GENERATOR	• Not controllable • multi-tone
	dc-to-RF EFFICIENCY	Cannot be optimized
	TX ANTENNA SPECS	• Directivity unknown • Polarization and position unknown • Multi-band sources
RADIO CHANNEL	RF-to-RF EFFICIENCY	• Unknown • Worst case (statistical) estimate
RECEIVER SIDE (RX)	RECTIFIER	Design as a compromise for a broad range of power densities and frequencies
	RF-to-dc EFFICIENCY	Can be optimized
	RX ANTENNA SPECS	• Non directive • Circularly or dual polarized • Multi-band resonant

Tab. I: EH system characteristics.

WIRELESS POWERING ON DEMAND		
TRANSMITTER SIDE (TX)	POWER GENERATOR	• high efficiency PA • optimized signal waveforms (multisine, UWB, chaotic signals)
	dc-to-RF EFFICIENCY	Can be optimized
	TX ANTENNA SPECS	• Directive • Defined polarization and position • Smart beaming is possible
RADIO CHANNEL	RF-to-RF EFFICIENCY	• Known • Optimized
RECEIVER SIDE (RX)	RECTIFIER	Design for specific power densities and RF frequencies, multistage topology
	RF-to-dc EFFICIENCY	Can be optimized
	RX ANTENNA SPECS	• Directive • Defined polarization and position • Single-band

Tab. II: Intentional WPT system characteristics.

Power transmission optimization challenges

In order to enable energy autonomy of a plethora of low-power wireless nodes located in ad-hoc positions, the focus for the power transmission subsystem is not only the maximization of the power source dc-to-RF efficiency, but also the maximization of the range to be covered with the minimum power density in the ambient. Indeed a smart power sorting can assist in keeping the possible lowest power density in the ambient, thus minimizing interference and EM pollution. We show that, once the transmitter efficiency maximization is ensured, by means of the vast number of technique available from the power amplifier design [10-13], the WPT transmitter capabilities can be augmented by a suitable real-time beaming technique to focus the transmitting antenna system in the direction of the devices to be powered. Furthermore, by adopting optimized multi-tone transmitted waveforms the receiver range can be enhanced by boosting the rectifier operation, especially at low input RF powers, thus increasing its RF-to-dc conversion efficiency. These two aspects are foreseen to be strategic ones for scenarios where the locations of the battery-less devices can be precisely determined so that the radio channel is known and the RF-to-RF efficiency can be exploited to minimizing the power density, without compromising the device operations.

Power beaming

A smart power beaming capability at the transmitter side can be of strategic importance in view of energy-aware WPT systems. For this purpose, time-modulated arrays (TMAs) have been

recently proposed in [14] for an energy-efficient and precise WPT procedure. The schematic representation of this kind of radiating system is given in Fig. 4(a): at the n antenna ports there are nonlinear RF switches, driven by periodical sequences of rectangular pulses ($bias_k(t)$, k=1,2,⋯,n) of period $T_M=1/f_M$ and amplitude V_{dd} (of the kind reported in Fig. 4(b) for the generic k-th switch). In this way, the radiation pattern of the RF carrier to be radiated (f_0), can be dynamically synthesised by acting on the on/off ratio of the switches excitation period [15], and also on the switch-on time instant [16, 17], thus creating an almost unlimited number of array control sequences. The control sequence of a 16-dipole array, reproducing a Dolph-Chebyshev excitation for side-lobe level reduction is given, as an example, in Fig. 5(a): Fig. 5(b) shows the corresponding radiation pattern at the fundamental frequency, with a side-lobe level of -30 dB. Note that TMAs also have a simpler architecture with respect to other beam forming solutions, such as phased-arrays [18] or retrodirective arrays [19]: in fact, they do not need for phase shifters in order to create the proper phase condition at the antenna ports.

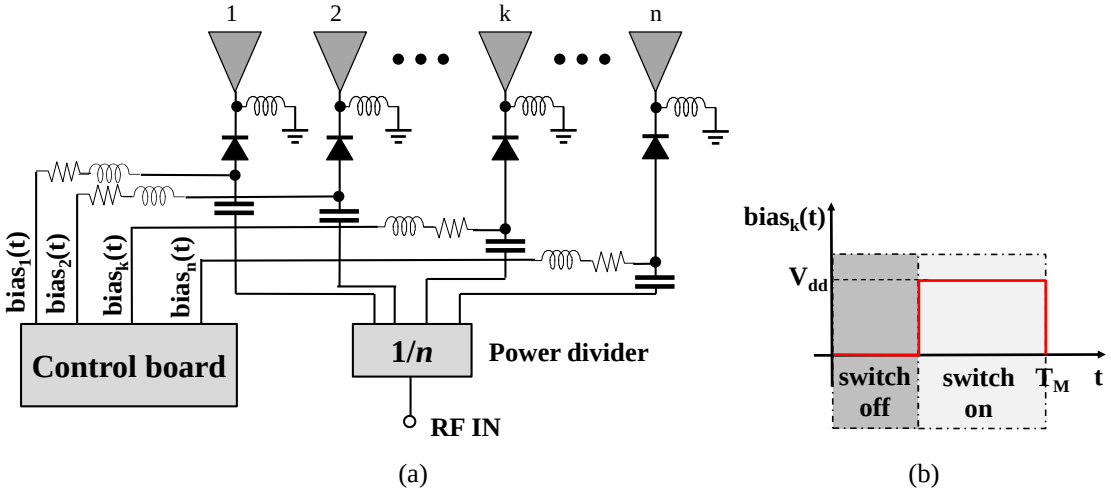

Fig. 4: (a) Schematic representation of a linear TMA with n radiating elements; (b) generic k-th element rectangular pulse for k-th antenna control.

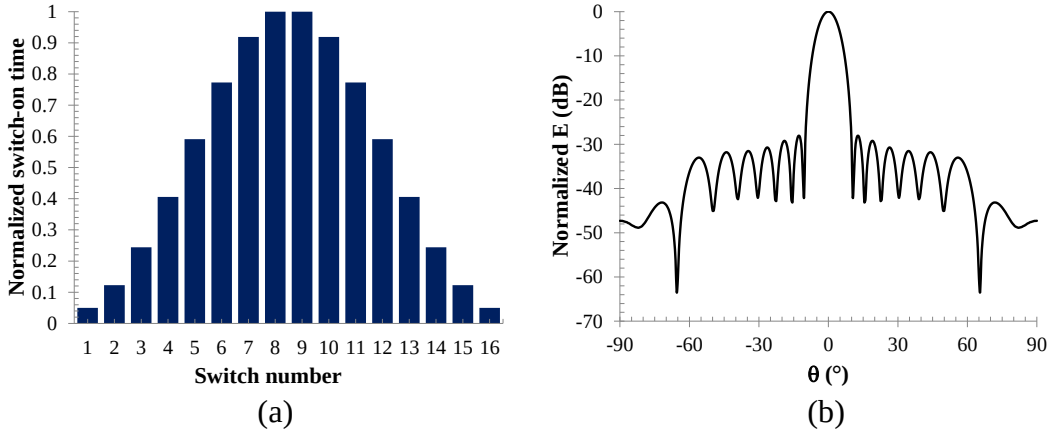

Fig. 5: (a) Normalized switch-on time of the 16 nonlinear switches of a dipole array reproducing a Dolph-Chebyshev pattern for side-lobe level control; (b) corresponding radiation pattern at the fundamental frequency with side-lobe level = -30 dB.

Due to the superposition of the periodic switch control sequences (with frequency f_M) with the RF carrier frequency f_0, TMAs are able to radiate not only at the fundamental carrier (f_0, h=0), but also at the sideband harmonics (f_0+hf_M, $h\neq0$). This property has been exploited in [14] for a

smart two-step WPT procedure via TMAs: first, a two-element time-modulated sub-array is used for localization of tagged sensors to be energized; then the entire TMA provides the power to the detected tags.

The TMA adopted in [14] for the smart WPT activity is the uniform 16-monopole planar array reported in Fig. 6: it operates at f_0 =2.45 GHz and is realized on a Taconic RF60A substrate (ε_r=6.15, thickness=0.635 mm). The spacing between the elements is the standard $\lambda/2$ distance. As switching elements, microwave Schottky diodes (Skyworks SMS7630-079) are used, driven by periodic sequences with modulation frequency f_M=100 kHz.

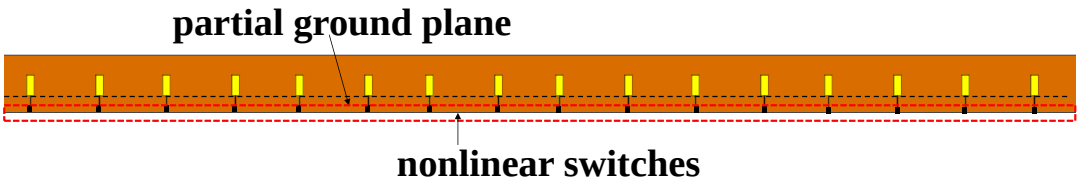

Fig. 6: Layout of the uniform 16 monopoles linear TMA [14].

Localization of the tags

In the first step of the WPT procedure the TMA is used for the detection of N tagged sensors. At this stage the 14 peripheral switches are left open, and the sole two-inner-element sub-array is operating. By piloting the two switches in the way indicated in Fig. 7(a) [20], it is possible to obtain the fundamental radiation pattern at f_0 with the sum (Σ) shape, while the first harmonic ones, at $f_0 \pm f_M$, reproduce the shape of the difference (Δ). By acting on the excitation duty-cycle (parameter δ) it is also possible to scan the Δ pattern in the way indicated in Fig. 7(b): with the two inner monopoles of the array of Fig. 6, a scanning region of about $\pm 60^\circ$ is achieved.

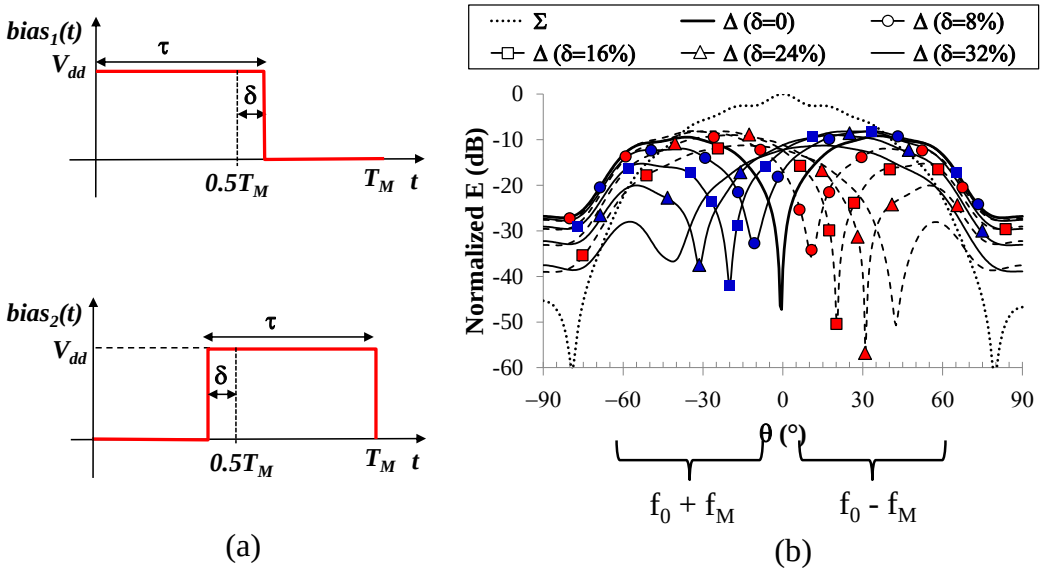

Fig. 7: (a) Control patterns of the two inner array elements switches providing Σ and Δ patterns; (b) corresponding simulated Σ and Δ radiation patterns for different δ values [14].

After a standard RFID reading operation for tags IDs acquisition, the sharpness of the negative peaks of the steered Δ patterns allows high resolution in the localization phase: this fact can be exploited by means of a suitable combination of the Received Signal Strength Indicators (RSSI)

backscattered by the tags, due to both the Σ and Δ patterns in order to build the Maximum Power Ratio (MPR) [21]:

$$MPR(\theta) = \Sigma_{RSSI}^{dB}(\theta) - \Delta_{RSSI}^{dB}(\theta) \quad (2)$$

The combination of the figure of merit (2) with the scanning capability has proven its effectiveness in indoor localization, with resolution up to few cm at 2.45 GHz [21]: the number of steps, discretizing the scanning window addressed in [21], is now realized by a proper number of switches control sequences, of the kind reported in Fig. 7(a).
At the end of the scanning activity a vector with the N values of θ corresponding to the peaks of the received MPRs (θ_{peak}) is recorded.

Transfer of power to tags

Once the tags position has been retrieved, the whole 16-element array of Fig. 6 is used, by adopting a control sequences involving all the switches and providing the desired power beaming behavior. One has to imagine to have preloaded the controller of the TMA switches with a list of control sequences able to manage different radiation patterns. In the present case, a possible decision rule during the WPT activity could be to split the scanning region ($\theta \in [-60^\circ \div 60^\circ]$) into sectors of amplitude equal to the half power beam width (HPBW) (7° in this case): for each θ_{peak} falling in the sector centered around θ_{HPBW}, The TMA controller loads the control sequence pointing the first harmonic to the θ_{HPBW} direction.
For instance, in case of a θ_{peak} falling in the sector centered around $\theta_{HPBW}=0^\circ$ the fixed fundamental harmonic beam can provide the energy to the corresponding sensor, while the two sideband harmonics ($h=\pm 1$) can be used to simultaneously energize another couple of symmetrically placed tags. Fig. 8(a) describes a possible solution in case of three detected tags falling inside the sectors $\theta_{HPBW} = -30^\circ, 0^\circ, 30^\circ$: the multi-beam performance are obtained by driving the switches with the control sequence reported in Fig. 8(b) [16], which represents the result of an optimization procedure, with specifications on the sideband beams pointing directions, as well as on their amplitudes. In this way the higher harmonic power peaks are only few dBs (~3 dB) below the fundamental one.

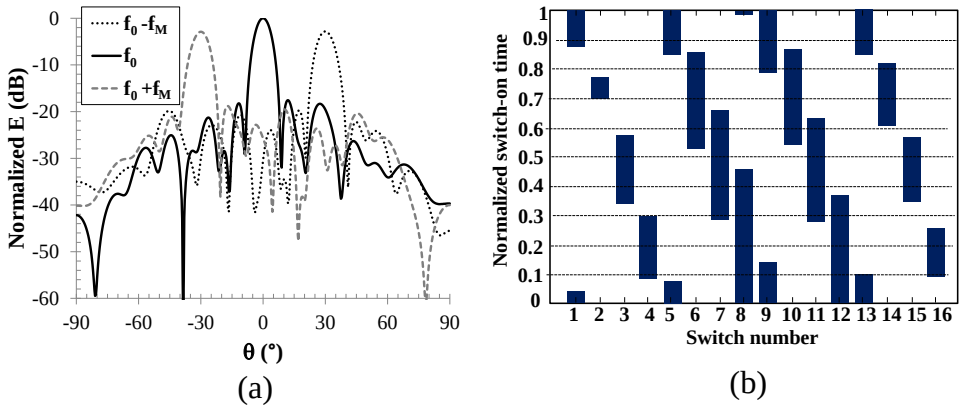

Fig. 8: (a) Fundamental and first sidebands radiation patterns of the 16-element array for the simultaneous power transfer in $\theta=-30^\circ, 0^\circ, 30^\circ$ directions [14], and (b) corresponding control sequence showing the normalized switch-on time of the 16 nonlinear switches [16].

Optimization of transmitted signal waveform

Recent studies [22-24] have demonstrated that rectifiers circuits designed to manage low RF input power, of the order of -20 dBm or less, improve their rectification performance when driven by multi-sine waveforms, with high peak-to-average power ratio (PAPR), in place of a CW signals with the same average power. In this way diode losses, due to turn-on voltage at low input powers can be overcome. It has to be noticed that to be effective, the multisine waveforms of such high-PAPR signal need be carefully designed to ensure the proper phase relationships which are responsible of the higher DC rectifier output: in the experiment of [23] voltage spikes occur when the tone are aligned in phase, as reported in Fig. 9 and this increases harvester efficiencies at low powers (typically less than 0 dBm) at the expense of bandwidth, whereas a decreased efficiency at high powers (typically greater than 0 dBm) is observed.

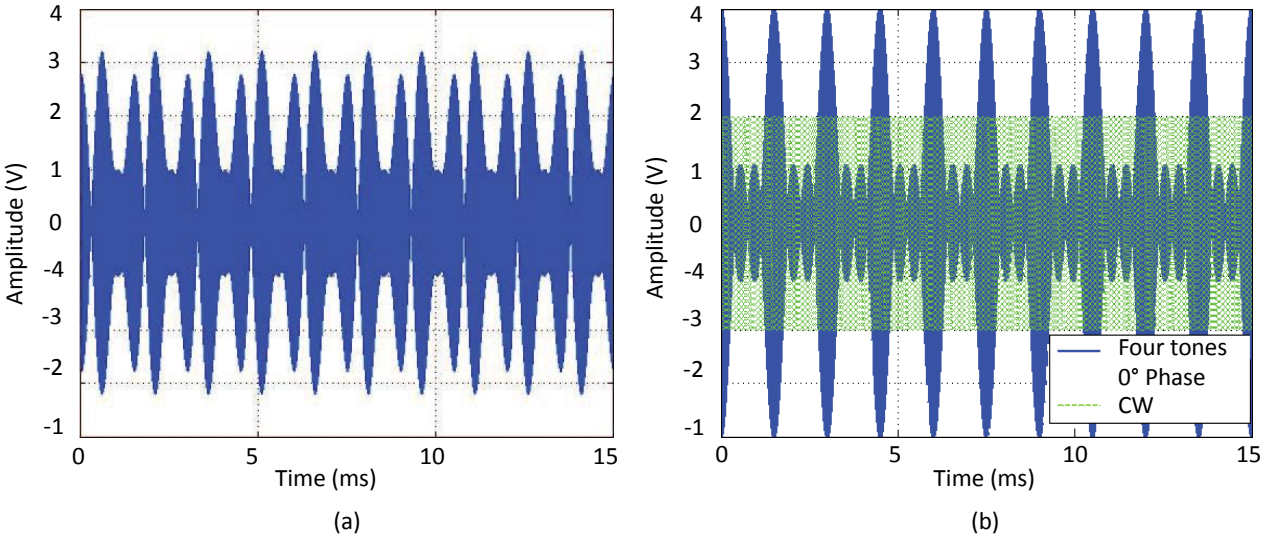

Fig. 9: Time-domain waveforms: (a) four-tone multisine with a random phase arrangement; (b) four-tone with 0° phase arrangement overlapped with a CW with the same average power [23].

Figs. 10(a,b) [23] shows the rectification outputs, in case of a single frequency excitation imposed on a diode I-V curve, of a CW and a high-PAPR signal with the same power. To fully exploit this promising technique the entire RF radio link need be controlled to ensure the proper phase relationships.

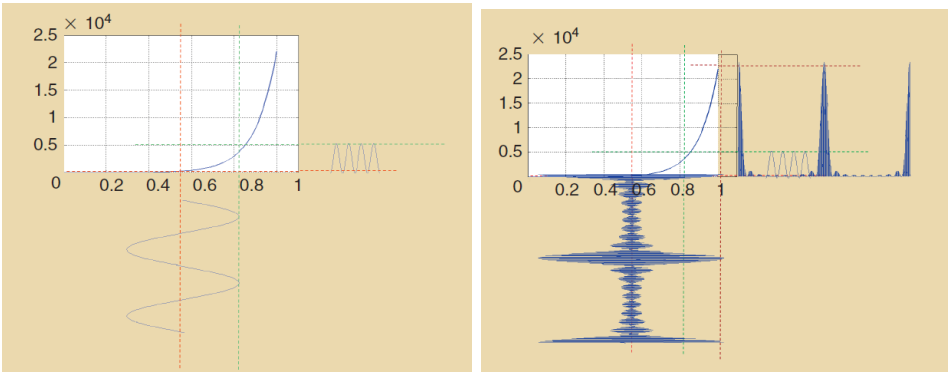

Fig. 10: Rectification of a sinusoidal signal (a), and of a high-PAPR multisine signal (b) (currents in μA and voltages in V) [23].

Different time domain waveforms, such as OFDM, white noise and chaotic waveforms, have been tested in [25] to assist the rectifier operations from the transmitter side, at received power levels up to 0 dBm. These experiments, reported in Fig. 11, confirmed that, due to the intrinsic high PAPR of such modulation formats, the efficiency is boosted of a quantity better than 15% for RF input power lower than −5 dBm. However, this technique is attractive only at low rectifier input power levels, and this is numerically and experimentally demonstrated in [26], although different modulation formats with respect to [25] are used. Fig. 12 reports the comparison of measured rectifier conversion efficiency at power levels spanning from 0 to 10 dBm for a CW and QPSK modulated signals with increasing bit rate. The efficiency degradation as input power increases worsens with increasing bit-rate due to the demand of a larger bandwidth. It is noteworthy that these power limits can vary with the rectifier topology and the diode-like devices adopted.

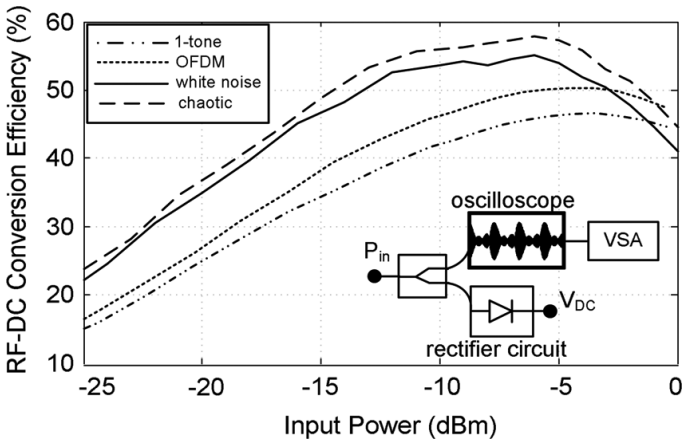

Fig. 11: RF-DC conversion efficiency of the rectifier circuit versus total input power for different test signals [25].

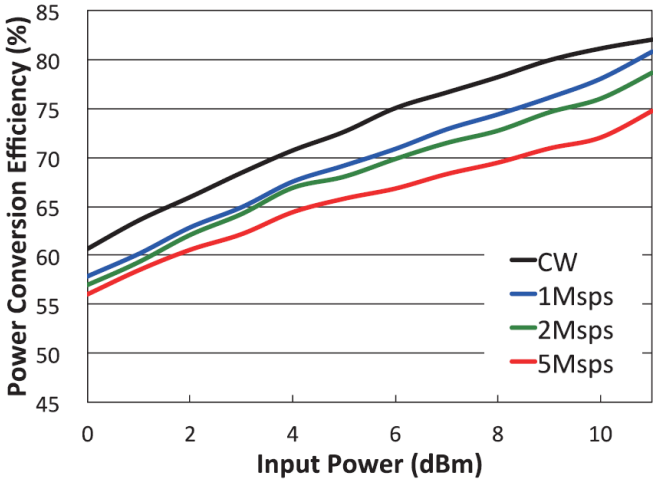

Fig. 12: Measured conversion efficiency of QPSK signals [26].

Receiver side: maximizing the received power

The low amounts of available RF power in real environments [5-9] has led to hybrid solutions for energy harvesters, exploiting the coexistence of different energy sources, besides the RF ones, as depicted in Fig. 13.

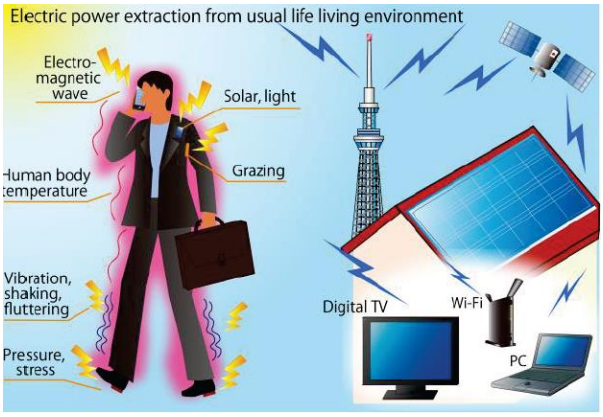

Fig. 13: Available environmental sources [27].

Vibrational energy is the additional source proposed in [28], while the planar rectenna area is exploited to host a photovoltaic cell in [29]. In [30] flexible fabrics show to be a suitable support for multiple scavenging transducers, deploying RF, solar and thermal sources. In all these solutions the cooperative action of different sources demonstrates an improvement in the total harvester conversion efficiency.

In practical energy harvesting applications, the final user of the power rectified by the rectenna is a device operating discontinuously, e.g. a sensor which needs to be activated in very short time intervals a few times per day. As a consequence, rectennas need for an intermediate energy buffer (or power management unit (PMU)) able to manage the variable workload conditions. Well-established solutions consist of dc-to-dc switching converters able to dynamically track the maximum power point (MPP) condition: an output rectified voltage of about one half of the open-circuit one has demonstrated to be close to the optimum condition, for any frequency and power level [31, 32].

The proper choice of the rectifier topology can significantly enhance the RF-to-dc conversion efficiency, too. For extremely low RF power budgets involved, the use of two Schottky diodes arranged in the single stage full-wave rectifier (or voltage doubler) topology shown in Fig. 14(a), has demonstrated to be the most convenient choice, because of the reduced diode losses [33]. An increase of the stages number can be justified only in different scenarios, such as in RFID tag applications, involving higher power levels, as demonstrated by Fig. 14(b).

The recent study in [34] has demonstrated a significant advantage in using backward tunnel diodes instead of traditional Schottky ones. Tunnel diodes based their operating principle on the quantum mechanical tunneling effect rather than the thermionic emission effect of the Schottky diodes. This has been proven to be sufficient to significantly increase the RF-to-dc conversion efficiency of a half-wave rectifier (single diode) prototype: measurements of RF-to-dc conversion efficiency at -40dBm/2.4GHz show that the backward diode outperforms the HSMS-285B Schottky diode by a factor of 10.5, and the Skyworks SMS 7630 by a factor of 5.5 [34].

However, one limiting factor for exploiting these diodes is the very high real part impedance observed in the UHF band (hundreds of Ω), which is not easy to be matched.

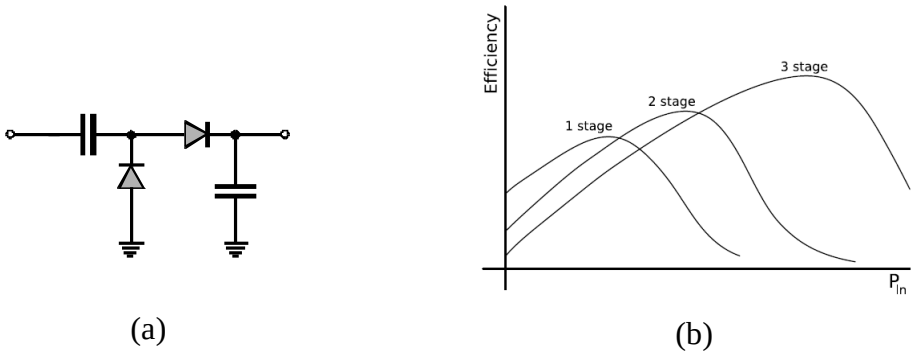

Fig. 14: Single stage full-wave rectifier topology (a); RF-to-dc efficiency behavior vs. input RF power, for different number of rectifying stages [33]

However, an energy autonomous subsystem is still an issue when ultra-low power densities are concerned. In the following we point out some of the recent novelties in rectenna design, which pave the way to the exploitation of RF scavengers in real scenarios.

Dual-mode rectifier

The main restriction in rectennas exploitation, even if operating in MPP condition, consists of the low values of the rectified voltages they typically provide, lower than the threshold voltage of diodes and transistors, and thus not able to wake-up the PMU.
A possible solution to this problem is proposed in [35], where a novel rectifier design approach tries to directly solve the problem at RF, instead at baseband. As described in Fig. 15, the antenna is loaded by a parallel connection of two matching network/rectifier assemblies: the lower one is optimized to operate during the start-up when extremely low voltages are involved, and the main goal is to reach the PMU wake-up condition, even if scarce RF-to-dc conversion efficiencies are achieved; the upper branch is devoted to standard MPP converter operation and is automatically used when a sufficient voltage level is guaranteed by the start-up phase.

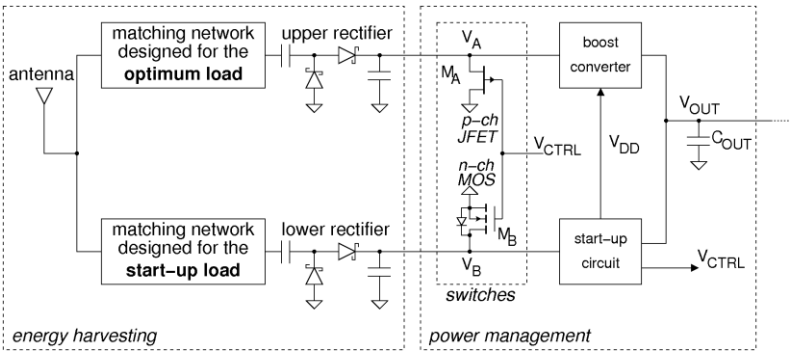

Fig. 15: Block diagram of the two-branch rectifier proposed in [35].

The complex design of the two-way rectifier can be accomplished by exploiting the highly different load conditions offered by the two operating regions, as explained in Fig. 16(a),

referring to a standard rectenna: an almost open-circuit load pertains to the start-up condition, in conjunction with the desired high dc voltage; a lower resistive load characterizes the second branch, together with higher conversion efficiency. In this way, two mutually-exclusive and alternatively well-matched paths represent the antenna load in the two operating conditions (upper and lower rectifiers in Fig. 15). It is noteworthy that, during the start-up step, the main goal is to reach the dc voltage needed to autonomously enable the dc-dc converter operation, regardless the poor conversion efficiency. Once this goal is reached, the start-up branch is automatically disconnected and the antenna load is provided by the upper rectifier. In this way the lower branch drains only a negligible amount of RF power

Fig. 16(b) demonstrates the feasibility of the proposed idea, by reporting a comparison of the measured average powers rectified by a standard rectifier and by the new two-branch rectifier, as a function of the incoming RF power level. In practice the novel solution assures the achievement of a fixed voltage level with half of the available RF power needed in the standard case.

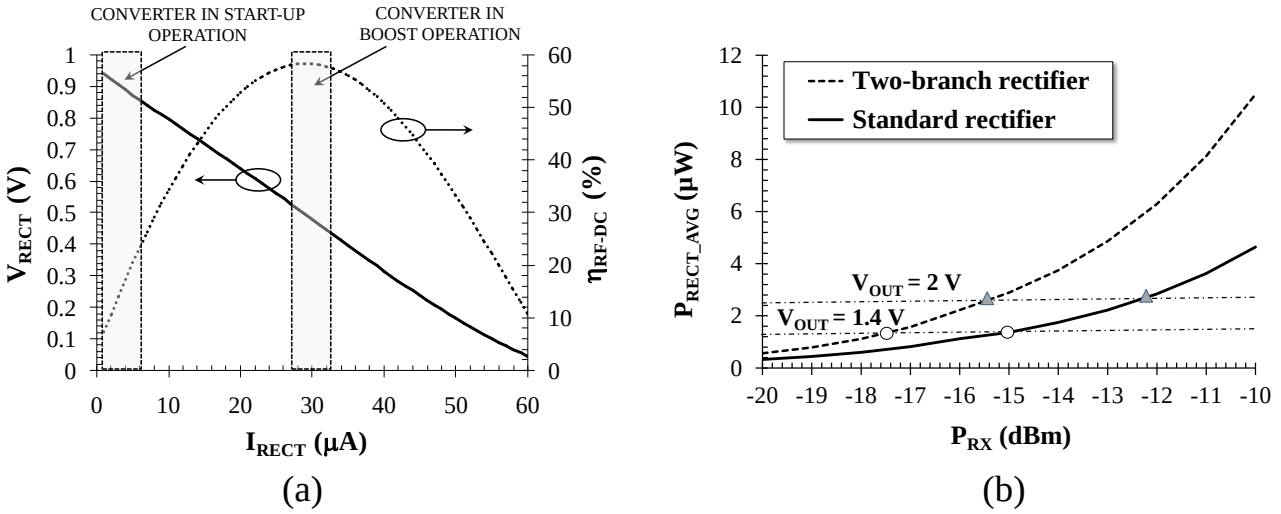

Fig. 16: (a) Optimized rectifier efficiency and output dc voltage as a function of the load current consumption (for P_{RX} = 25 μW); (b) average output dc power P_{RECT_AVG} versus input power P_{RX} in case of dual-branch and of conventional single-branch rectifier (both loaded with the start-up circuit) [35].

Resistance compression networks

Typically a rectifying circuit is designed to provide the maximum RF-to-dc efficiency for a given fixed load and signal level. As previously stated, this represents a limitation with respect to the actual rectifier operating conditions for a two-fold point of view: i) the nonlinear behavior of the rectifier is strongly dependent on the RF available power provided by the receiving antenna; ii) the actual rectifier load is a dc-to-dc converter, as depicted in Fig. 1, representing a variable load impedance, changing, for instance, with the charging level of the storage capacitor. For these reasons the design of the rectenna matching network becomes a demanding task, due to the highly variable impedance offered by the rectifier.

An interesting solution to this problem is proposed in [36] by means of a new class of matching networks, called resistance compression networks, that greatly reduces the variation of the

effective resistance seen at their input port as loading impedance changes. The simple linear circuits of Fig. 17 represent two (dual) solutions of this kind of networks, exploiting reactive branches: here R represents the real load varying across a wide range, whereas X is a specified reactance offered by the two branches, with identical amplitudes and opposite phases, at the designed operating frequency.

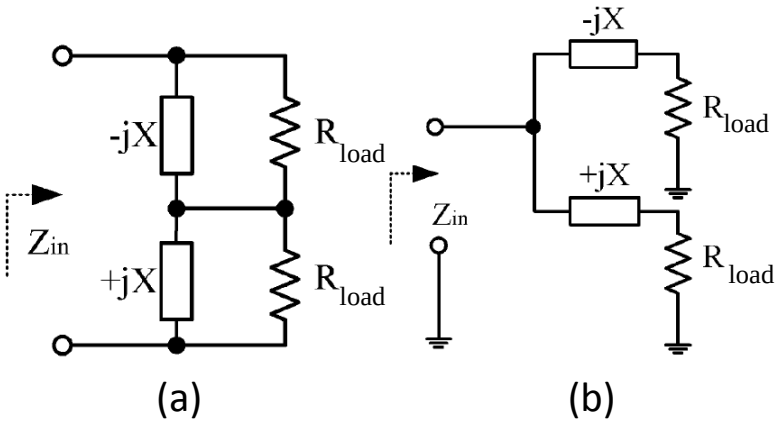

Fig. 17: Structure of two basic resistance compression networks [36].

The relationships between the input resistance (R_{in}) and the load (R_{load}) is given by the simple formulas:

$$R_{in\_a} = \frac{2R_{load}}{1+\left(\frac{X}{R_{load}}\right)^2} \quad ; \quad R_{in\_b} = \frac{X^2}{2R_{load}}\left[1+\left(\frac{R_{load}}{X}\right)^2\right] \tag{3}$$

where the subscripts a and b stand for the cases of Fig. 17(a) and (b), respectively, and the compression of the load resistances is around a center value equal to X.

A practical limitation in the use of compression networks in energy harvesting applications (see Tab. I) is the need for wideband or multiband solutions for a complete coverage of the available wireless standards (as discussed in next pages): the amplitude and phase conditions on the reactance X should be valid at all the rectenna operating frequencies.

To overcome this problem in [37] a dual-band compression network of the kind of Fig. 17(b), operating at 915 MHz and 2.45 GHz, is proposed and realized. The topology shown in Fig. 18 shows the adopted solution, providing the required opposite phase condition by using networks with reversed input and output ports in the two branches. Fig. 19 demonstrates the comparison between the dual-band rectifier of Fig. 18 and a standard rectifier, optimized at the two frequency bands: the advantage of the new solution both in terms of load resistance (Fig. 19(b)) and input power variations (Fig. 19(d)) is evident.

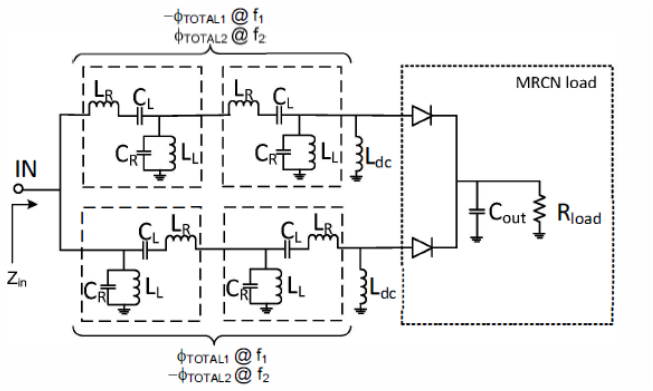

Fig. 18: Schematic of the rectifier circuit with multi-band resistance compression network [37].

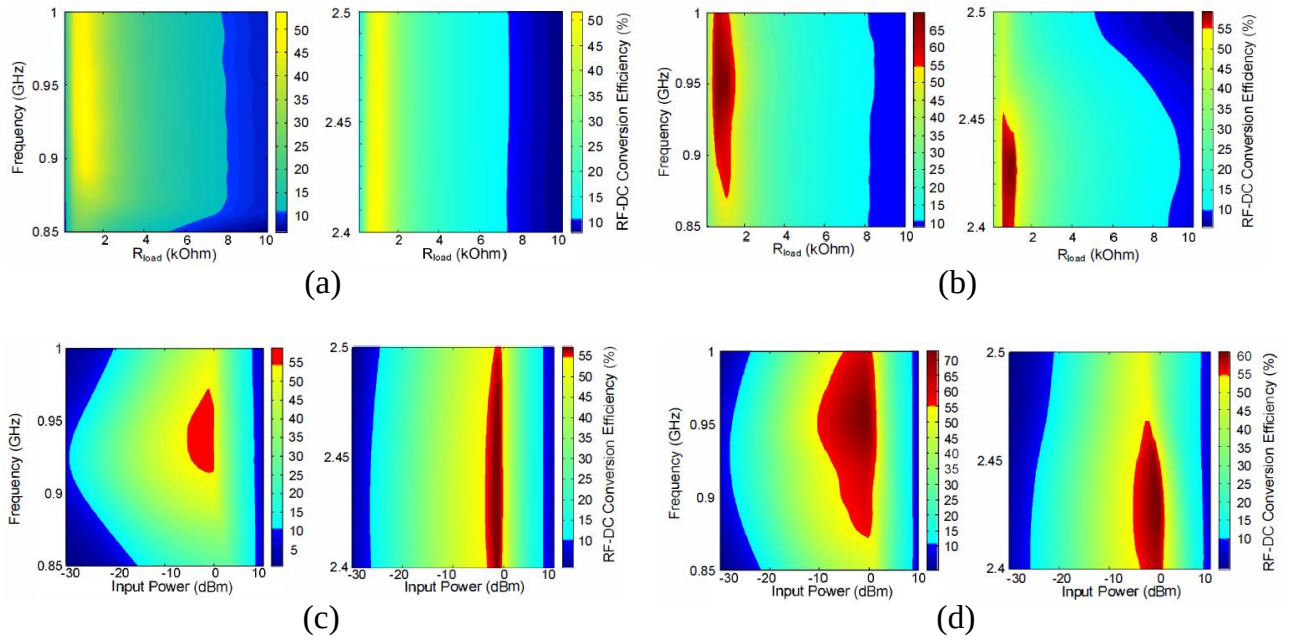

Fig. 19: RF-to-dc conversion efficiency: for an input power of 0 dBm (a) of the single-diode rectifier and (b) of the new dual-band rectifier ; for R_{load}=1 kΩ (c) of the single-diode rectifier and (d)of the new dual-band rectifier [37].

Wideband and Multi-band rectification

The low amount of RF available power in realistic humanized scenarios [5-9] has led the researchers to deploy the presence of multiple sources at different frequencies: the use of wideband or multi-band antennas in energy harvesting applications is widely diffused in the literature. A multi-band or multi-resonant antenna can be preferable for the higher radiation efficiency, since at the resonance the antenna provides the best radiation efficiency [38, 39]. However antennas exploiting the auto-similarity principle [40], such as Archimedean or log-periodic spiral antennas, represent a wideband solution with optimum performance [41].

The design of such a kind of rectenna can represent a highly complex task, for the reasons explained in the previous paragraph, but also for the dispersive behavior of the antenna itself. An electromagnetic description of the antenna is mandatory for an accurate design of the whole system, but represents an additional variable parameter to be taken into account in the design of

the multi-frequency matching network, for a multi-level incoming signal. The solution to this problem is to design the harvester as a whole, including both the RF-to-dc converter and the PMU, as described in Fig. 20: here the standard dc-to-dc converter (PC), for MPP tracking operation, is sustained by a start-up unit (SU) for wake-up operation, in order to improve the performance of a tri-band wearable harvester, deploying the available wireless sources at 900, 1800, 2450 MHz [42].

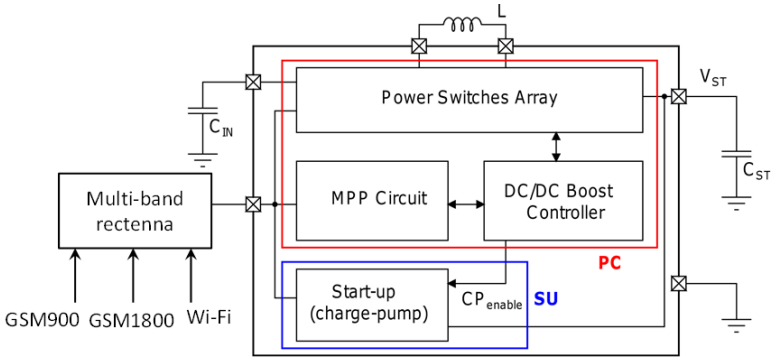

Fig. 20: Block diagram of the whole EH system deploying a tri-band rectenna [42].

A multi-source source solution can be fruitful from another point of view: the nonlinear nature of the rectifying circuit is advantageous in the simultaneous presence of different sinusoidal (or modulated) signals, since the high number of intermodulation frequency products due to the diodes nonlinearities can be rectified, too, thus increasing the RF-to-dc conversion efficiencies. This is demonstrated by Figs. 21, 22 for a multi-band [43] and a wideband rectenna [41], respectively. Fig. 21 reports the simulated rectified voltages, on an fixed 900 Ω load placed at the output port of a textile tri-band rectenna, resulting from superposition of different sources (line with circles) and from single source at a time, as a function of the power transmitted by a resonant half-wavelength dipole. The transmitted power values of the figure are associated to one excitation in the single-tone analyses and are equally distributed among the different tones in the multi-tone case. It is worth noting that the advantage from intermodulation distortion is significant at lower P_{TX} levels, typical of harvesting scenarios, and becomes negligible at higher power due to the nonlinear behavior of the diode, for the same reasons discussed in the previous session on optimized transmitted waveforms.

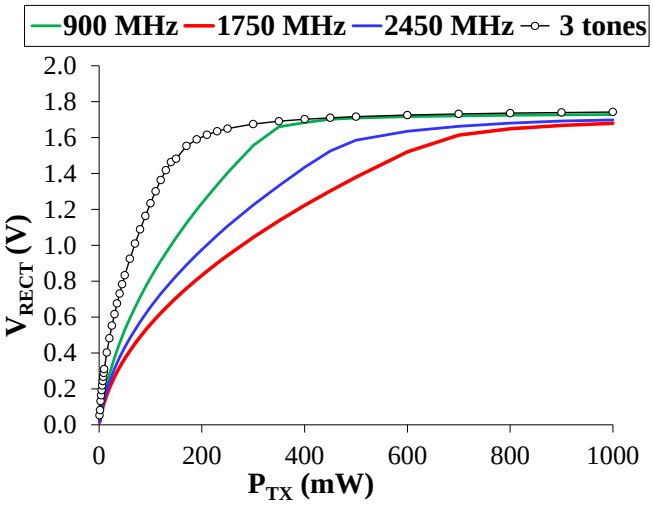

Fig. 21: dc output voltage of a tri-band wearable rectenna in stationary single-tone and multi-

tone regime [43].

Fig. 22 shows similar results for a log-periodic spiral antenna [41]: the comparison of the total rectified power for independent and simultaneous dual-frequency illumination for 10,000 randomized input pairs of frequency sources falling in the 2-8 GHz band. The mean increase due to the contemporaneous presence of RF sources is always significant.

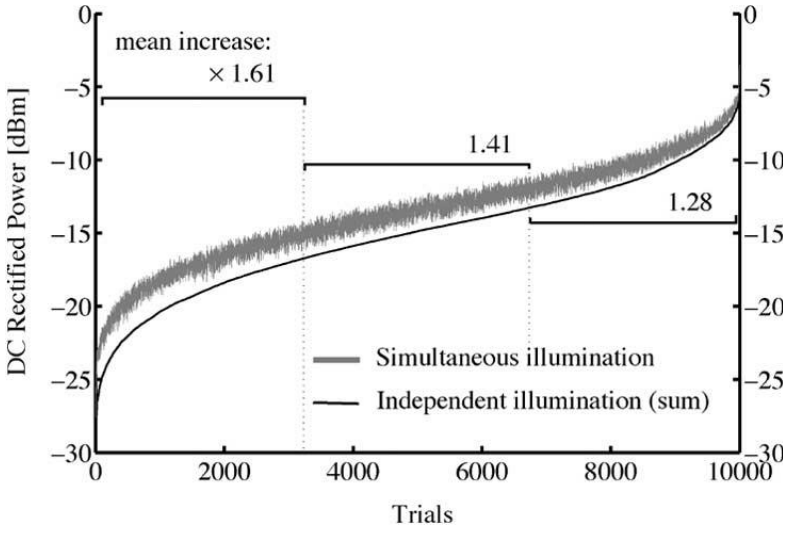

Fig. 22: Comparison of total rectified power for independent and simultaneous dual-frequency illumination [41].

Bi-directional wireless relay-node

In view of a seamless reconfiguration of architectures based on wireless devices, it is of great interest to rely on devices integrating both RF energy harvesting and wireless power transfer capabilities, thus acting on demand either as a user or as a wireless power provider. If such devices operate bi-directionally to exploit themselves the harvested power or to act as power relay nodes, with the highest possible conversion efficiency, they can be used to provide energy to randomly but closely located wireless devices. In this way such wireless devices can be dynamically relocated counting on these power relay nodes. The power relay nodes allow thus to maximize both η_{RF-RF} and η_{RF-DC} in (1), due to their bidirectional use.

A promising solution for this strategic node is presented in [44], where it is demonstrated that class-F RF power amplifiers, for medium power transfer (on the order of a few watts), exhibit comparable efficiencies when operated as self-synchronous rectifiers. In [45], this concept is extended to a 2.14-GHz 85% efficient 10-W class-F^{-1} rectifier. A reconfigurable class-E oscillator/rectifier in the UHF band is detailed in [46] for RF power in the mW range. In both operating states, high conversion efficiencies are obtained for specific gate and drain dc biases, a limiting factor for system operation.

In [47] a novel circuit solution is presented, with bidirectional functionality and, most of all, without the need for external batteries: it makes use of the energy stored during the rectifier operation mode to act as a repeater. The same nonlinear circuit performs the two operations, where two switches are simultaneously driven to position 1 for oscillator operation, and to position 2 for rectifier operation, as described in Fig. 23(a). The main novelties of this solution are: i) implementation of self-biasing of the transistor [48] for proper oscillator class-F

operation; and ii) increased efficiency in the rectifier mode at low input power levels by means of a bias-assisting feedback loop. In this way the circuit does not need a dedicated gate bias supply, and thus eliminates on-board batteries, enabling a completely energy-autonomous device with high efficiency in both transmit and power-receive modes.

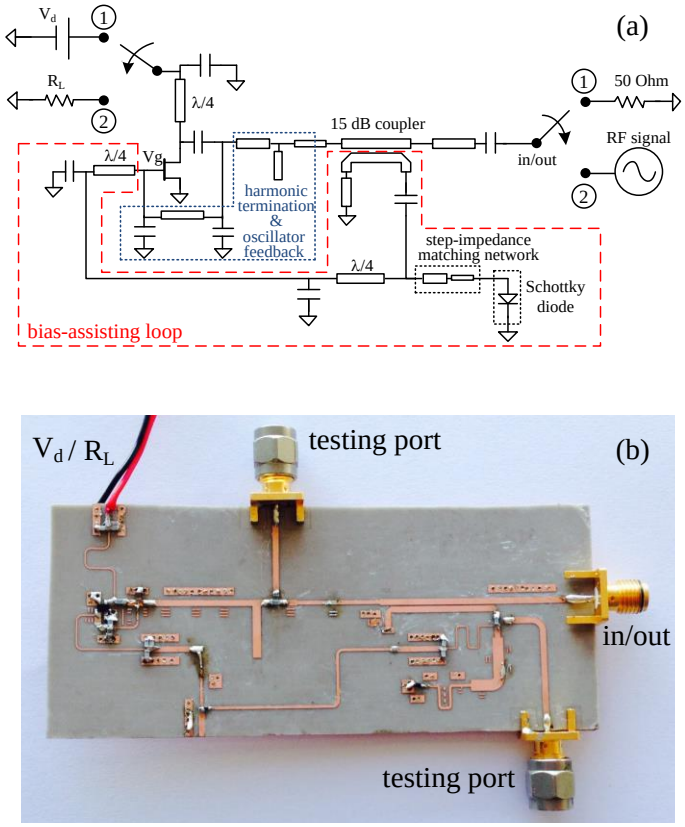

Fig. 23: Oscillator/rectifier circuit with bias-assisting feedback loop: (a) schematic of the circuit, (b) photo of the fabricated prototype [47].

The performance of the prototype shown in Fig. 23(b) are summarized in Fig. 24. Fig. 24(a) shows the output power and dc-to-RF conversion efficiency of the circuit operating as an oscillator as a function of drain supply voltage. It can be observed that the efficiency remains above 50% over most of the drain supply range. The oscillator mode has a maximum dc-to-RF conversion efficiency of 55.6% at 4.8 V drain bias voltage and an output power of 12 dBm. Fig. 24(b) shows the measured RF-to-dc conversion efficiency, in rectifying mode, as a function of input power. The plots show that the circuit is able to operate with efficiency higher than 45% starting from as low as -4 dBm of input power. This performance is preserved over a 22 dB range in input power. The circuit is able to operate even at lower input power levels but with reduced efficiency (20% efficiency for -10 dBm input power).

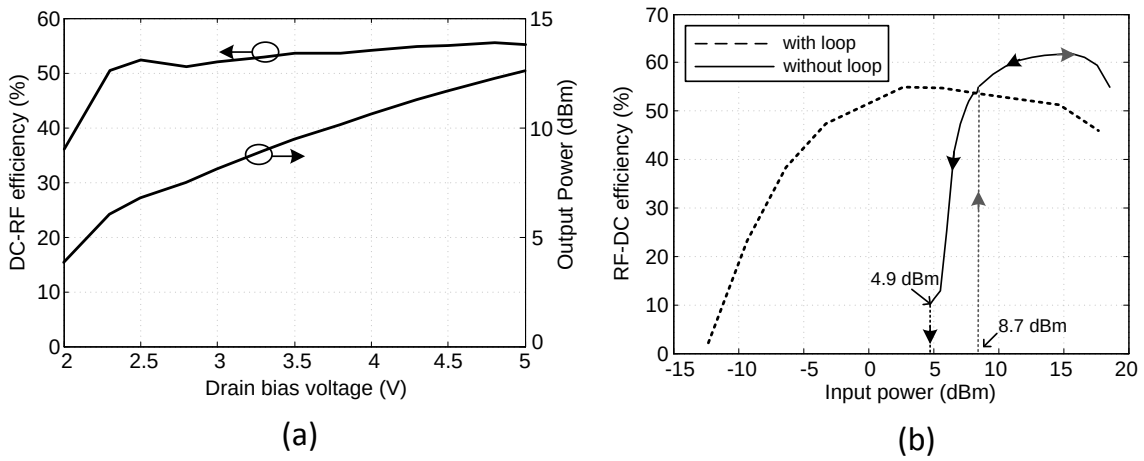

Fig. 24: (a) Measured output power and dc-to-RF efficiency of the oscillator/rectifier circuit operating in oscillator mode; (b) measured RF-to-dc conversion efficiency for the oscillator/rectifier circuit operating in rectifier mode [47].

Conclusion

In this article we have considered some of the most recent RF/microwave circuital and signaling solutions to assist wireless powering of maintenance-free devices and to take a step forward in the reliable implementation of co-operative smart spaces. This is currently one of the deepest need in the widespread world of pervasive monitoring, including, but not limited to, ambient assisting living, structural monitoring, e-health, agriculture and risk working environment. In such scenarios low-duty cycle, low-power (tens of μW) wireless sensors nodes are adopted, possibly realized in eco-friendly material and without batteries. Ambient RF energy harvesting has been successfully demonstrated to comply with these requirements, but due to its strong environment-dependent performance and its intermittent availability is not foreseen to be a robust solution. On the contrary dedicated RF sources providing power on demand, with optimized densities and time interval operations, is foreseen as a more reliable choice. It has already been proven that, by a concurrent optimization of the transmitter and the receiver side, both interference and EM pollution can be kept under control. At the transmitter side, smart beaming, combined with real time localization techniques, can be coupled with optimized power waveforms to ensure, at the receiver side, successful operation of a rectifier, with input power as low as -10 dBm.

At the wireless node side, it has been demonstrated that nodes switchable between rectifier and power generator can autonomously operate starting at -10 dBm with an efficiency of 20% and can be exploited for providing/extracting power to/from the closely located devices, thus cooperating with the smart environment to ensure the energy autonomy balance.

References

[1] D. Spenza, M. Magno, S. Basagni, L. Benini, M. Paoli, C. Petrioli, "Beyond duty cycling: Wake-up radio with selective awakenings for long-lived wireless sensing systems," *2015 IEEE*

Conference on Computer Communications (INFOCOM), pp.522-530, April -May 2015.
[2] Z. Popovic, E.A. Falkenstein, D. Costinett, R. Zane, "Low-Power Far-Field Wireless Powering for Wireless Sensors," *Proceedings of the IEEE*, vol.101, no.6, pp.1397-1409, June 2013.
[3] A. Costanzo, M. Dionigi, D. Masotti, M. Mongiardo, G. Monti, L. Tarricone, R. Sorrentino, "Electromagnetic Energy Harvesting and Wireless Power Transmission: A Unified Approach," *Proceedings of the IEEE*, vol.102, no.11, pp. 1692-1711, Nov. 2014.
[4] V. Rizzoli, A. Costanzo, D. Masotti, P. Spadoni, and A. Neri, "Prediction of the End-to-End Performance of a Microwave/RF Link by means of Nonlinear/Electromagnetic Co-Simulation ", *IEEE Transactions on Microwave Theory and Techniques,* Vol. 54, No. 12, Dec. 2006, pp. 4149-4160.
[5] H.J. Visser, A.C.F. Reniers, J.A.C. Theeuwes, "Ambient RF Energy Scavenging: GSM and WLAN Power Density Measurements," *38th European Microwave Conference*, pp.721-724, Oct. 2008.
[6] M. Pinuela, P.D. Mitcheson, S. Lucyszyn, "Ambient RF Energy Harvesting in Urban and Semi-Urban Environments," *IEEE Trans. Microwave Theory Tech.,* vol. 61, no. 7, pp. 2715-2726, July 2013.
[7] R.J. Vyas, B.B. Cook, Y. Kawahara, M.M. Tentzeris, "E-WEHP: A Batteryless Embedded Sensor-Platform Wirelessly Powered From Ambient Digital-TV Signals," *IEEE Transactions on Microwave Theory and Techniques*, vol.61, no.6, pp.2491-2505, June 2013.
[8] A. N. Parks, A.P. Sample, Y. Zhao, J.R. Smith, "A wireless sensing platform utilizing ambient RF energy," 2013 IEEE Topical Conf. on Biomedical Wireless Techn, Networks, and Sensing Systems (BioWireleSS), pp.154-156, Jan. 2013.
[9] Z. Popovic, "Cut the Cord: Low-Power Far-Field Wireless Powering," *IEEE Microwave Magazine,* vol.14, no.2, pp.55-62, March-April 2013.
[10] A. Zai, Li Dongxue, S. Schafer, Z. Popovic, "High-efficiency X-band MMIC GaN power amplifiers with supply modulation," *2014 IEEE MTT-S International Microwave Symposium (IMS),* pp.1-4, June 2014.
[11] Y. Kobayashi, M. Hori, H. Noji, G. Fukuda, S. Kawasaki, "The S-band GaN-based high power amplifier and rectenna for space energy transfer applications," *2012 IEEE MTT-S International Microwave Workshop Series on Innovative Wireless Power Transmission: Technologies, Systems, and Applications (IMWS),* pp.271-274, 10-11 May 2012.
[12] M. Thian, A. Barakat, V. Fusco, "High-Efficiency Harmonic-Peaking Class-EF Power Amplifiers With Enhanced Maximum Operating Frequency," *IEEE Transactions on Microwave Theory and Techniques,* vol.63, no.2, pp.659-671, Feb. 2015.
[13] G. Nikandish, E. Babakrpur, A. Medi, "A Harmonic Termination Technique for Single- and Multi-Band High-Efficiency Class-F MMIC Power Amplifiers," *IEEE Transactions on Microwave Theory and Techniques,* vol.62, no.5, pp.1212-1220, May 2014.
[14] D. Masotti, R. Marchukov, V. Rizzoli, A. Costanzo, "Far-field power transmission by exploiting time-modulation in linear arrays," *2015 IEEE Wireless Power Transfer Conference (WPTC),* pp.1-4, 13-15 May 2015.
[15] W. H. Kummer, A. T. Villeneuve, T. S. Fong, F. G. Terrio, "Ultra-low sidelobes from time-modulated arrays", *IEEE Transactions on Antennas & Propagation*, vol.AP-11, no. 6, pp. 633-639, Nov. 1963.

[16] L. Poli, P. Rocca, G. Oliveri, A. Massa, "Harmonic beamforming in time-modulated linear arrays through particle swarm optimization", *IEEE Transactions on Antennas & Propagation*, vol. 59, no. 7, pp. 2538-2545, July 2011.
[17] S. Yang, Y. B. Gan, A. Qing, and P. K. Tan, "Design of a uniform amplitude time-modulated linear array with optimized time sequences," *IEEE Transactions on Antennas & Propagation*, vol. 53, no. 7, pp. 2337-2339, July, 2005.
[18] T. Takahashi, T. Mizuno, M. Sawa, T. Sasaki, T. Takahashi, N. Shinohara, "Development of phased array for high accurate microwave power transmission," *2011 IEEE MTT-S International Microwave Workshop Series on Innovative Wireless Power Transmission: Technologies, Systems, and Applications (IMWS),* pp.157-160, May 2011.
[19] R.T. Iwami, A. Zamora, T.F. Chun, M.K. Watanabe, W.A. Shiroma, "A retrodirective null-scanning array", *2010 IEEE MTT-S International Microwave Symposium Digest,* pp.81-84, May 2010.
[20] A. Tennant, B. Chambers, "A Two-Element Time-Modulated Array With Direction-Finding Properties," *IEEE Antennas and Wireless Propagation Letters*, vol. 6, pp. 64-65, 2007.
[21] M. Del Prete, D. Masotti, N. Arbizzani, A. Costanzo, "Remotely Identify and Detect by a Compact Reader With Mono-Pulse Scanning Capabilities," *IEEE Transactions on Microwave Theory and Techniques*, vol.61, no.1, pp. 641-650, Jan. 2013.
[22] A.S. Boaventura, N.B. Carvalho, "Maximizing DC power in energy harvesting circuits using multisine excitation," *2011 IEEE MTT-S International Microwave Symposium Digest,* pp.1-4, June 2011.
[23] A. Boaventura, D. Belo, R. Fernandes, A. Collado, A. Georgiadis, N. Borges Carvalho, "Boosting the Efficiency: Unconventional Waveform Design for Efficient Wireless Power Transfer," *IEEE Microwave Magazine*, vol. 16, no. 3, pp. 87-96, April 2015.
[24] C.R. Valenta, G.D. Durgin, "Rectenna performance under power optimized waveform excitation," *2013 IEEE International Conference on RFID (RFID)*, Apr. 30-May 2 2013, pp. 237-244.
[25] A. Collado, A. Georgiadis, "Optimal Waveforms for Efficient Wireless Power Transmission," *IEEE Microwave and Wireless Components Letters,* vol.24, no.5, pp.354-356, May 2014.
[26] H. Sakaki, T. Kuwahara, S. Yoshida, S. Kawasaki, K. Nishikawa, "Analysis of rectifier RF-DC Power Conversion Behavior with QPSK and 16 QAM input signals for WiCoPT system," *2014 Asia-Pacific Microwave Conference (APMC),* pp.603-605, Nov. 2014.
[27] M. Kawashima, T. Nakamura, K. Hata, "Construction of healthcare network based on proposed ECG and physical-activity sensor adopting energy-harvesting technologies," *2013 IEEE 15th International Conference on e-Health Networking, Applications & Services (Healthcom),* pp.31-35, Oct. 2013.
[28] C.H.P. Lorenz, S. Hemour, W. Liu, A. Badel, F. Formosa, K. Wu, "Hybrid Power Harvesting for Increased Power Conversion Efficiency," *IEEE Microwave and Wireless Components Letters,* in press.
[29] K. Niotaki, A. Collado, A. Georgiadis, Kim Sangkil, M.M. Tentzeris, "Solar/Electromagnetic Energy Harvesting and Wireless Power Transmission," *Proceedings of the IEEE* , vol.102, no.11, pp.1712-1722, Nov. 2014.
[30] S. Lemey, F. Declercq, H. Rogier, "Textile Antennas as Hybrid Energy-Harvesting Platforms," *Proceedings of the IEEE* , vol.102, no.11, pp.1833-1857, Nov. 2014.

[31] A. Dolgov, R. Zane, Z. Popovic, "Power Management System for Online Low Power RF Energy Harvesting Optimization," *IEEE Transactions on Circuits and Systems I: Regular Papers,* vol. 7, no. 7, pp. 1802-1811, July 2010.
[32] A. Costanzo, A. Romani, D. Masotti, N. Arbizzani, and V. Rizzoli, "RF/baseband co-design of switching receivers for multiband microwave energy harvesting," *Sensors and Actuators A: Physical*, vol. 179, pp. 158-168, Jun. 2012.
[33] J. Essel, D. Brenk, J. Heidrich, and R. Weigel, "A highly efficient UHF RFID frontend approach," *IEEE MTT-S International Microwave Workshop on Wireless Sensing, Local Positioning, and RFID (IMWS 2009)*, pp. 1-4, Sept. 2009.
[34] C.H.P. Lorenz, S. Hemour, W. Li, Y. Xie, J. Gauthier, P. Fay, K. Wu, "Overcoming the efficiency limitation of low microwave power harvesting with backward tunnel diodes," *2015 IEEE MTT-S International Microwave Symposium (IMS),* pp.1-4, May 2015.
[35] D. Masotti, A. Costanzo, P. Francia, M. Filippi, A. Romani, "A Load-Modulated Rectifier for RF Micropower Harvesting With Start-Up Strategies," *IEEE Transactions on Microwave Theory and Techniques*, vol. 62, no. 4, pp. 994-1004, April 2014.
[36] Han Yehui, O. Leitermann, D.A. Jackson, J.M. Rivas, D.J. Perreault, "Resistance Compression Networks for Radio-Frequency Power Conversion," *IEEE Transactions on Power Electronics,* vol.22, no.1, pp.41-53, Jan. 2007.
[37] K. Niotaki, A. Georgiadis, A. Collado, "Dual-band rectifier based on resistance compression networks," *2014 IEEE MTT-S International Microwave Symposium (IMS),* pp.1-3, 1-6 June 2014.
[38] D. Masotti, A. Costanzo, M. Del Prete, V. Rizzoli, "A Genetic-Based Design of a Tetra-Band High-Efficiency RF Energy Harvesting System", *IET Microwaves Antennas & Propagation*, Vol. 7, no. 15, 2013, pp. 1254 - 1263.
[39] V. Kuhn, C. Lahuec, F. Seguin, C. Person, , "A Multi-Band Stacked RF Energy Harvester With RF-to-DC Efficiency Up to 84%," *IEEE Transactions on Microwave Theory and Techniques,* vol.63, no.5, pp.1768-1778, May 2015.
[40] W. Wiesbeck, G. Adamiuk, C. Sturm, "Basic Properties and Design Principles of UWB Antennas," *Proceedings of the IEEE*, Vol. 97 , no. 2, 2009, pp. 372 - 385, Feb. 2009.
[41] J.A. Hagerty, F.B. Helmbrecht, W.H. McCalpin, R. Zane, Z.B. Popovic, "Recycling ambient microwave energy with broad-band rectenna arrays," *IEEE Transactions Microwave Theory and Techniques*, vol. 52, no. 3, pp. 1014-1024, March 2004.
[42] M. Dini, M. Filippi, A. Costanzo, A. Romani, M. Tartagni, M. Del Prete, D. Masotti, "A fully-autonomous integrated rf energy harvesting system for wearable applications," *2013 European Microwave Conference (EuMC),* pp.987-990, 6-10 Oct. 2013.
[43] A. Costanzo, D. Masotti, "Wirelessly powering: An enabling technology for zero-power sensors, IoT and D2D communication," *2015 IEEE MTT-S International Microwave Symposium (IMS),* pp.1-4, May 2015.
[44] T. Reveyrand, I. Ramos, Z. Popović, "Time-reversal duality of high-efficiency RF power amplifiers," *Electronics Letters*, vol.48, no.25, pp.1607,1608, Dec 2012.
[45] M. Roberg, T. Reveyrand, I. Ramos, E. Falkenstein, Z. Popovic, "High-Efficiency Harmonically Terminated Diode and Transistor Rectifiers," *IEEE Transactions Microwave Theory and Techniques,* vol. 60, pp. 4043-4052, Dec. 2012.
[46] M.N. Ruiz, A. Gonzalez, R. Marante, J.A. Garcia, "A reconfigurable class E oscillator/rectifier based on an E- pHEMT," *Integrated Nonlinear Microwave and Millimetre-Wave Circuits (INMMIC),* 2012 Workshop on, pp.1,3, 3-4 Sept. 2012.

[47] M. del Prete, A. Costanzo, A. Georgiadis, A. Collado, D. Masotti, Z. Popovic, "Energy-autonomous Bi-directional Wireless Power Transmission (WPT) and energy harvesting circuit," *2015 IEEE MTT-S International Microwave Symposium (IMS),* pp.1-4, 17-22 May 2015.
[48] H. Abe, "A GaAs MESFET Self-Bias Mode Oscillator (Short Paper)," *IEEE Transactions Microwave Theory and Techniques*, vol.34, no.1, pp.167,172, Jan. 1986.